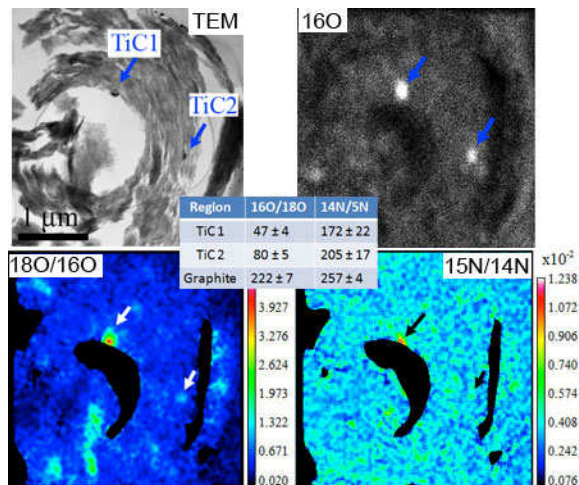


**ISOTOPICALLY-EXTREME INCLUSIONS AND ISOTOPIC HETEROGENEITY IN SUPERNOVA GRAPHITIC SPHERULES.** T. K. Croat and F. Gyngard, Laboratory for Space Sciences and Department of Physics, Washington University, St. Louis, MO 63130, USA, tkc@wustl.edu.

**Introduction:** Isotopic measurements of refractory grains captured within graphitic spherules often exhibit extreme anomalies, which in some cases lead to a different understanding of the stellar origin of the assemblage (e.g., the presence of type-C SiC grains of massive star origin in high-density graphites [1]). NanoSIMS imaging measurements also show isotopic heterogeneities, as a function of both spatial distribution and depth, which can reveal complex condensation histories of supernova (SN) graphite spherules [2]. However, the interpretation of data from SN assemblages is complicated by isotopic dilution/exchange and by their multiphase nature -each spherule can contain hundreds of small refractory grains. Here we present NanoSIMS data from cross-sections of SN graphite spherules, and examine the isotopic heterogeneity of both the host graphites and their internal refractory grains.

**Experimental:** Graphitic spherules from the Murchison KE3 (1.65-1.72 g cm<sup>-3</sup>, >2 μm [3]) and Orgueil OR1d (1.75-1.92 g cm<sup>-3</sup>, >1 μm [4]) density and size separates were selected for ultramicrotomy based on NanoSIMS bulk measurements indicative of a SN origin. The ultramicrotomed graphite cross-sections were studied in the TEM, primarily using imaging, EDXS, and electron diffraction. Selected graphite cross-sections were then measured in NanoSIMS imaging mode for various species of interest, including <sup>12</sup>C<sup>-</sup>, <sup>13</sup>C<sup>-</sup>, <sup>16</sup>O<sup>-</sup>, <sup>17</sup>O<sup>-</sup>, <sup>18</sup>O<sup>-</sup>, <sup>12</sup>C<sup>14</sup>N<sup>-</sup>, <sup>12</sup>C<sup>15</sup>N<sup>-</sup>, <sup>28</sup>Si<sup>-</sup>, <sup>29</sup>Si<sup>-</sup>, and <sup>30</sup>Si<sup>-</sup>. The NanoSIMS standards used include fine-grained Murchison matrix, synthetic SiC, and carbon-coated TEM grids, and the reported 2σ errors include reproducibility variations in the standards. In a few cases, graphite cross-sections that happened to fall on TEM gridbars were measured, and here the TiC locations are apparent based on the high initial <sup>16</sup>O<sup>-</sup> yield from TiCs [5].

**Results:** Internal TiC grains from SN graphites often show significant <sup>15</sup>N and <sup>18</sup>O enrichments, typically larger than the host graphite (Fig. 1). Even without prior knowledge of their locations, the TiCs are apparent in the earlier layers of <sup>16</sup>O images, due to differences in initial secondary ion yields (Fig.1). The TiCs in Fig. 1 are 130 and 80 nm in diameter, although they appear ~50% larger in NanoSIMS images due to lower spatial resolution in the ion probe compared to the TEM. The average sizes of TiCs vary among different SN graphites, but these range from 30-250 nm [6]. Only the smallest TiC (<50 nm) are difficult to detect



**Fig. 1.** TEM image of a KE3e15 SN graphite cross-section containing two TiC grains with corresponding <sup>16</sup>O image and ratio images of <sup>18</sup>O/<sup>16</sup>O and <sup>15</sup>N/<sup>14</sup>N showing hotspots at the same TiC locations. The TiCs have significantly larger <sup>18</sup>O and <sup>15</sup>N enrichments than their graphite host (see inset data table with 2σ errors).

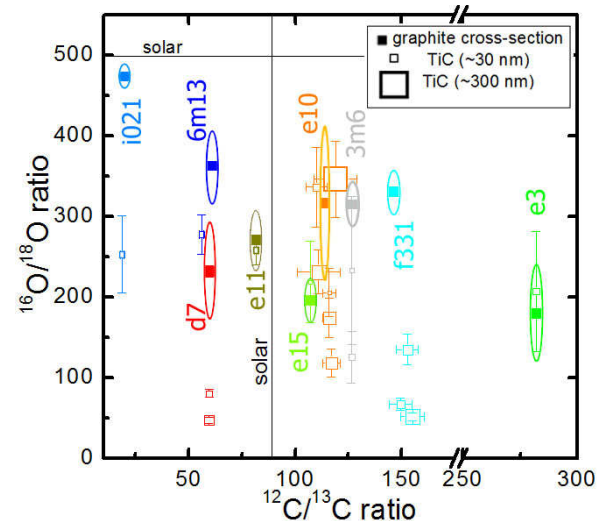


**Fig. 2.** <sup>12</sup>C/<sup>13</sup>C vs. <sup>16</sup>O/<sup>18</sup>O plots of TiC inclusions (open symbols of various sizes) and their graphite host (closed symbols and range indicated by ellipses) from nine SN graphite spherules. The TiC symbols share the same color as their graphite host and are scaled to reflect the sizes of each TiC inclusion measured.

and measure; here ion counts from the surrounding ~70 nm thick graphite cross-section begin to obscure any isotopic differences between the TiCs and the host graphite. Fig. 2 shows <sup>12</sup>C/<sup>13</sup>C and <sup>16</sup>O/<sup>18</sup>O ratios from

nine different OR1d and KE3 SN graphite cross-sections along with measurements from their TiC inclusions (each TiC is plotted in same color as its host). The TiC plot symbols are scaled relative to the TiC's size, and measurements of the smaller subgrains are more greatly affected by contributions from surrounding graphite (i.e., pulled towards host graphite isotopic range). Graphitic carbon regions are isotopically heterogeneous and the ellipses in Fig. 1 show the isotopic range of TiC-free areas. In most cases, the TiCs are clearly more  $^{18}\text{O}$  enriched than their graphite host, but are similar in  $^{12}\text{C}/^{13}\text{C}$  (irrespective of TiC size). Only the smallest single TiC grains, such as those in graphites e11 and e3 (Fig. 2) are isotopically indistinguishable from graphite. However, even in those cases, the aggregate isotopic anomalies from TiCs (i.e., computed by combining counts from  $\sim 10$  TiCs) exceeds those of their host graphite.

Fig. 3 shows the  $^{12}\text{C}/^{13}\text{C}$  and  $^{16}\text{O}/^{18}\text{O}$  ratios as a function of radial distance from the graphite's center from various representative SN spherules (with the innermost to outermost shells computed separately). The  $^{16}\text{O}/^{18}\text{O}$  ratios typically show radial isotopic zoning, with the innermost region being most anomalous and the outermost shell showing closer to solar ratios. The  $^{12}\text{C}/^{13}\text{C}$  ratios sometimes show similar isotopic zoning patterns, but are generally much less affected. No features such as the  $^{18}\text{O}$ -enriched shell in [2] were seen, but other radial trends are often seen that indicate changing condensation condition in the gas (e.g., in chemical composition and/or number of TiCs captured [6]). We also find some evidence for isotopic hetero-

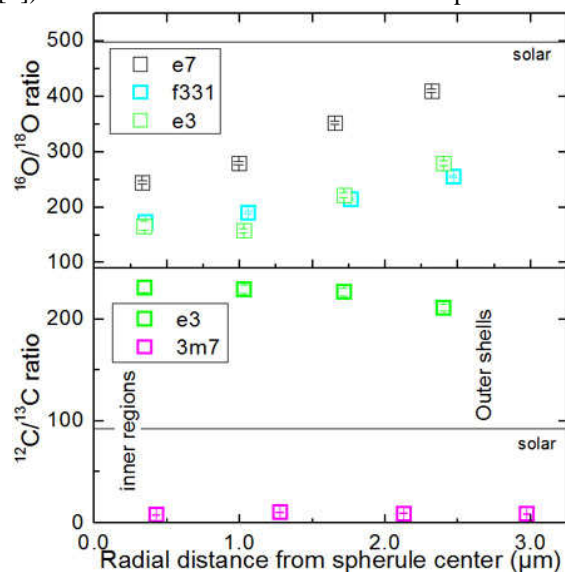


Fig. 3.  $^{12}\text{C}/^{13}\text{C}$  and  $^{16}\text{O}/^{18}\text{O}$  isotopic zoning profiles from various TiC-free cross-sections taken near each spherule's center. The inner region gives the spherule's core composition and the remaining three data points are from concentric shells further outward.

geneity among TiCs from the same graphitic spherule (e.g., e10 in Fig. 2).

**Discussion:** The SN TiCs have significant N distributed throughout the grains (up to 10 at. %) and have O concentrated at their surfaces [7], and so are more accurately described as Ti-carbonitriles. The large  $^{15}\text{N}$  and  $^{18}\text{O}$  anomalies in TiCs are both consistent with formation in regions dominated by material from the He/C SN zone [2], rather than having an origin from deep within the SN [8]. Ca-Ti isotopic measurements (looking for  $^{44}\text{Ca}$  or  $^{49}\text{Ti}$  excesses) are being pursued to further constrain their origins.

The isotopic differences between TiCs and their host graphite raise the possibility that they have condensed from different environments. A more likely explanation, though, is that the graphitic carbon is more greatly affected by isotopic dilution and exchange of minor elements (e.g., N and O) than TiC, as suggested by the isotopic zoning patterns (Fig. 3). Such isotopic exchange occurs to an even greater degree in high-density graphites, which often retain only the C anomalies that are embedded into the graphene sheets that comprise their structures, but lose N and O that is more loosely bound at the edges of these sheets [1]. The anomalous N and O species appear to be better retained by the Ti-carbonitrile phase. Further, some evidence for the co-formation of TiCs and their host graphites in the same environment is apparent in their microstructures. For example, in some cases the TiC grains captured in a graphitic spherule are larger at greater radial distance from the graphite's center, which suggests continued TiC growth in the same environment where the spherules are growing [6].

The isotopic heterogeneity within graphitic spherules and the presence of more isotopically anomalous inclusions illustrate the difficulties in characterizing these multiphase assemblages. Here, measurements from ultramicrotomed cross-sections have a clear advantage over bulk measurements. Along with providing samples for TEM analyses, the cross-sections also allow a less ambiguous determination of the isotopic composition of the spherule's core, which more closely reflects its original true composition.

**Acknowledgments:** We thank S. Amari, M. Jadhav, and E. Groopman for assistance in preparation and characterization of the Murchison and Orgueil low-density graphite samples.

**References:** [1] Croat T.K. et al. (2010), *AJ*, 139, 2159. [2] Groopman E. et al. (2014) *ApJ*, 790: 9. [3] Amari S. et al. (2014) *GCA*, 133, 479. [4] Jadhav M. et al. (2013) *GCA*, 133, 193. [5] Stadermann F.J. et al. (2005) *GCA*, 69, 177. [6] Croat T.K. et al. (2003), *GCA*, 67, 4705. [7] Daulton T.L. et al. (2012) *LPSC* 53, # 2247. [8] Lodders K. *ApJ*, 647, L37.